Similitude of Scour around Bridge Piers

Oscar Link[1], and *Bernd* Ettmer[2]

[1] Civil Engineering Department, Universidad de Concepción, Chile
[2] Civil Engineering Department, Magdeburg University of Applied Sciences, Germany

Abstract. Scales involved in bridge pier scour include the Reynolds number, the Froude number, and the ratio of the pier to the sediment diameter, among others. Consequently, it is not possible to achieve perfect similitude, and thus scale effects between model and prototype arise. In fact, these scale effects distort the scour estimations typically used in hydraulic design of bridges, as scour formulas are based mainly on results from scour experiments at the laboratory scale. In this paper, proper scales of the flow, sediment, and scour are derived theoretically. The suitability of these scales to achieve perfect similitude of scour is tested through carefully designed laboratory experiments conducted in three different flumes having different sizes and piers of different diameters, with five bed materials of different sizes and densities. Results show that the dimensionless effective flow work, W* is a suitable criteria for scaling the effects of river flows on the local scour process around a pier in a bed composed by grains represented by the dimensionless grain diameter D*. In this context, scale effects of the ratio of the pier to the sediment diameter is quantified and shown to be negligible.

1. Introduction

Current practice in bridge pier design is based on the application of scour formulas that, on one side, provide results significantly different from each other [16] introducing important uncertainties in the design procedure, and, on the other side, are only applicable to bridges with few known pier geometries and configurations of pier groups. Alternatively to the application of scour formulas, river models with movable bed provide valuable information on prototype fluvial processes that can be difficult to obtain in the field or with mathematical techniques [17, 6]. Similitude between the prototype and model relies on equating dimensionless parameters for the flow and sediment transport, thus preserving consistent ratios of the dominant forces [18]. However, maintaining similitude between movable bed laboratory models and the larger rivers they represent is difficult, and typically scale effects arise. The estimation of how scale effects qualitatively and quantitatively affect the model results and whether or not they can be neglected is up to now a challenge for physical modelers [8, 9]. Until now a set of controlling parameters of bridge scour allowing the scalability of the process is not known [2].

Raudkivi [14] presented the functional trends of scour. At piers aligned with a steady flow in uniform sediments the relative scour depth, $Z^* = z/D$ (z is the maximum scour depth around the pier and D is the pier diameter) primarily depends on the flow intensity,

$I = u/u_c$ with u the section-averaged flow velocity and u_c the critical velocity for the initiation of sediment motion, the relative flow depth to pier diameter, $\hat{h} = h/D$ with h the flow depth, and the relative size of the pier to sediment D/d_s. The effect of the flow intensity on scour was recently investigated by [5] highlighting differences in scour produced under the clear-water condition $I < 1.0$, live-bed with bed-forms $1.0 \le I < 4.0$, and entrainment into suspension $I \ge 4.0$. [12] distinguished between narrow and wide piers, according to the relative flow depth to pier diameter $\hat{h}$, with negligible effects of $\hat{h}$ on Z* for $\hat{h} \ge 1.5$. [10] showed that equilibrium scour depth, Z^*_{eq} strongly depends on the relative size of the pier to sediment, with Z^*_{eq} increasing logarithmically with $D/d_s < 25$, and decreasing to $Z^*_{eq} \approx 1.3$ for $D/d_s > 400$. [3,4] analyzed the scale effects on scour concluding that the use of laboratory flumes in developing accurate predictors of scour depth at full-scale piers is limited due to scale effects that may produce greater scour depths Z^* at the laboratory than at actual piers in rivers.

Following dimensional analysis and developing ad-hoc laboratory experiments, the controlling scales for physical modeling of the bridge pier scour are deduced, and scale effects in distorted models are quantified.

2. Dimensional analysis and similitude

Scour depth at a cylindrical bridge pier in a homogeneous sediment bed depends on variables characterizing the fluid, flow, sediment, and pier. In functional form:

$$f(\mu, \rho, u_{ef}, h, g, d_s, \rho_s, D, t, z) = 0 \tag{1}$$

where *f* is a function, μ is the fluid dynamic viscosity; ρ is the fluid density; u_{ef} is the effective flow velocity; h is the flow depth at the undisturbed flow region; g is the gravitational acceleration; d_s is the representative sediment particle diameter; ρ_s is the density of a sediment particle; D is the pier diameter; t is the time, and z is the scour depth. For the particular case of scour around a cylinder the effective flow velocity, u_{ef} corresponds to the excess velocity above the incipient scour condition $u_{ef} = u - u_{cs}$, with u the section averaged flow velocity, and u_{cs} the critical velocity for the incipient scour. According to the π-Buckingham theorem, the set of ten independent variables could be reduced to seven non-dimensional parameters. Taking ρ_s, u_{ef}, and d_s as repeating variables:

$$f\left(\mathrm{R}', \mathrm{F}', \rho', \frac{h}{d_s}, \frac{D}{d_s}, \frac{u_{ef} t}{d_s}, \frac{z}{d_s}\right) = 0 \tag{2}$$

where $\mathrm{R}' = (u_{ef} d_s)/\nu$ is the effective particle Reynolds number; $\mathrm{F}' = u_{ef}/\sqrt{g d_s}$ is the effective particle Froude number; $\rho' = (\rho_s - \rho)/\rho$ is the relative density; h/d_s is the relative flow depth to sediment size; D/d_s is the relative size of the pier to sediment; $(u_{ef} t)/d_s$ is an unsteady parameter; and z/d_s is the relative scour depth to sediment size. Proper combination of dimensionless parameters in equation (2) leads to:

$$f\left(D^*, \mathrm{F_d}, \rho', \hat{h}, \frac{D}{d_s}, U^*, Z^*\right) = 0 \tag{3}$$

where $D^* = \left(R'^2/\left(F'^2/\rho'\right)\right)^{1/3} = \left(\rho' g/\nu^2\right)^{1/3} d_s$ is the dimensionless grain diameter representing sediment mobility; $F_d = F'\rho'^{-0.5} = u_{ef}/\sqrt{\rho' g d_s}$ is the effective, densimetric Froude number representing flow capacity to produce scour; $U^* = 2\left(u_{ef}t/d_s\right)\left(D/d_s\right)^{-2} = u_{ef}t/\left(D^2/\left(2d_s\right)\right) = u_{ef}t/z_R$ is a flow unsteadiness parameter with $z_R = D^2/\left(2d_s\right)$ a reference length proposed by [7], $\hat{h} = \left(h/d_s\right)\left(D/d_s\right)^{-1} = h/D$ is the relative flow depth; and $Z^* = \left(z/d_s\right)\left(D/d_s\right)^{-1} = z/D$ is the normalized scour depth.

Perfect similitude between model and prototype is achieved if all parameters in equation (3) are identic. Difficulties arise, however, for finding model sediments that satisfy this restriction when working with water at ambient temperatures, as model sediments are typically lighter and coarser than prototype sediments (e.g. [1]).

Recent results by [11, 13] suggest that the effective dimensionless work by the flow on the sediment bed surrounding a bridge pier comprises the effects of the unsteady parameter U^*, and the effective Froude number F_d, allowing to overcome the difficulties arising in achieving perfect similitude according to equation (3). The dimensionless, effective flow work is:

$$W^* = F_d^3 U^* = F_d^3 \frac{u_{ef} t}{(D^2/2d_s)} = \int_0^{t_{end}} F_d^3 \frac{u_{ef}}{(D^2/2d_s)} dt \tag{4}$$

where t_{end} refer to the duration of the hydrograph. Here u_{ef} can be a function of time. Moreover, if the analysis is restricted to cases where $\hat{h} > 1.5$ then Z^* becomes independent of the relative flow depth [12, 14]. Assuming that the effects of ρ' are well captured in F_d and D^*, then Z^* is approximated as:

$$Z^* \cong f\left(W^*, D^*, \frac{D}{d_s}\right) \tag{5}$$

According to equation (5), which is a simplified version of equation (2), similitude of the pier scour is achieved when the three controlling parameters are similar in model and prototype: $\lambda_{Z^*} \cong \lambda_{W^*} \cong \lambda_{D^*} \cong \lambda_{D/d_s} \cong 1$, with $\lambda_{Z^*} = Z_m^*/Z_p^*$, $\lambda_{W^*} = W_m^*/W_p^*$, $\lambda_{D^*} = D_m^*/D_p^*$, $\lambda_{D/d_s} = \left(D/d_s\right)_m/\left(D/d_s\right)_p$, where subindex m and p stand for model and prototype, respectively.

2.1. Experimentation

Experiments were conducted within three different flumes. Flume 1 consisted of an in-floor rectangular flume of 26 m long, 1.4 m wide and 0.74 m deep with a Plexiglass cylinder of diameter D = 0.15 m. Scour was measured in a non-intrusive manner from inside the pier with a laser distance sensor. Only clear-water experiments could be conducted in flume 1. Flume 2 consisted of a rectangular flume of 6.0 m long, 0.4 m wide and 0.4 m deep having a Technyl A® cylinder of diameter 0.046 m. Scour was monitored with a snake video camera having 7 mm in diameter that penetrated the free surface less than 1 cm, and recorded the sediment bed position on a graduation at the pier front, with a precision of ±0.5 mm. A sediment recirculation system in Flume 2 was used for live-bed experiments. Flume 3 consisted of a flume of 8.0 m long, 0.3 m in wide and 0.6 m in depth with a HDPE cylinder of 0.03 m in diameter. Scour was measured with a point gauge. Sediment recirculation was possible, thus Clearwater as well as live bed experiments could be

conducted. Flume 1 and Flume 2 are located at the Hydraulic Engineering Laboratory of the University of Concepción, Chile, while Flume 3 is located at the Leichtweiß-Institut für Wasserbau of the Technische Universität Braunschweig, Germany.

Four sediments and two other materials of different sizes and densities were used in the scour experiments. Table 1 shows the properties of the bed material, d_s is the sediment size taken as the sediment size for which 50% by weight is finer, d_{50}, σ_g is the standard deviation of the sediment particles size, and FF is the sediment shape factor.

Table 1. Properties of the bed material

	d_s (mm)	σ_g (-)	ρ_s (kg m^{-3})	FF (-)	D^* (-)
Sand 1	0,36	1,45	2650	0,70	9
Sand 2	0,74	1,18	2650	0,70	18
Sand 3	0,80	1,30	2650	0,70	21
Sand 4	1,60	1,29	2650	0,70	40
Acetal	2,60	1,00	1390	0,71	41
Polystyrene	2,74	1,05	1040	0,75	20

A total of 17 experimental runs classified into five series were conducted to test the reliability of the theoretically derived scales, as shown in Table 2.

Table 2. Experimental runs

Series	Exp	Flume	Sediment	u_B (ms^{-1})	h_B (cm)	u_p (ms^{-1})	t_p (min)	Duration (min)
S1	1	Flume 1	Sand 1	0.120	21.0	0.290	100	120
S1	2	Flume 1	Sand 1	0.120	21.0	0.290	20	120
S2	1	Flume 2	Sand 2	0.150	9.2	0.270	190	390

S2	2	Flume 1	Polystyrene	0.038	30.0	0.110	190	390
S2	3	Flume 2	Sand 2	0.150	9.2	0.420	25	50
S2	4	Flume 1	Polystyrene	0.038	30.0	0.170	25	50
S3	1	Flume 3	Sand 4	0.320	10.0	0.320	-	1440
S3	2	Flume 3	Acetal	0.210	10.0	0.210	-	1440
S3	3	Flume 2	Sand 2	0.260	9.2	0.260	-	1368
S3	4	Flume 1	Polystyrene	0.100	30.0	0.100	-	1351
S4	1	Flume 2	Sand 2	0.330	9.2	0.330	-	1444
S4	2	Flume 2	Sand 2	0.200	9.2	0.200	-	2988
S4	3	Flume 1	Polystyrene	0.125	30.0	0.125	-	1483
S4	4	Flume 1	Polystyrene	0.075	30.0	0.075	-	2321
S5	1	Flume 2	Sand 1	0.210	7.5	0.210	-	1350
S5	2	Flume 1	Sand 1	0.290	23.0	0.290	-	5172
S5	3	Flume 3	Polystyrene	0.110	7.2	0.110	-	190

In the table, u is flow velocity, h is flow depth, t is time, and the subindex “B” and “P” stay for base and peak discharge conditions.

Series S1 included experiments with variable discharge imposing a bell shaped hydrograph for testing the reliability of the dimensionless flow work, W* as a predictor of caused by a flood wave in a given material, thus representing the flow scale in pier scour problems. The second series S2 included experiments with variable discharge imposing a sinusoidal shape hydrograph with similar values of W* using different sediments with similar D*, to test the feasibility of D* for representing the sediment bed in the pier scour problem under clear-water and live-bed conditions. Figure 1 shows the hydrographs and corresponding dimensionless, effective flow work on time for experiments of series S1 and S2. Series S3 included experiments with steady discharge conducted until advanced stages of scour, and thus achieving high final values of W* on different sediments with similar D*, to test the reliability of the derived scales for modelling conditions close to equilibrium scour. Series S4 included additional experiments with steady discharges, having sediments with similar D*, but different ratios of d_s/D to evaluate scale effects in distorted models.

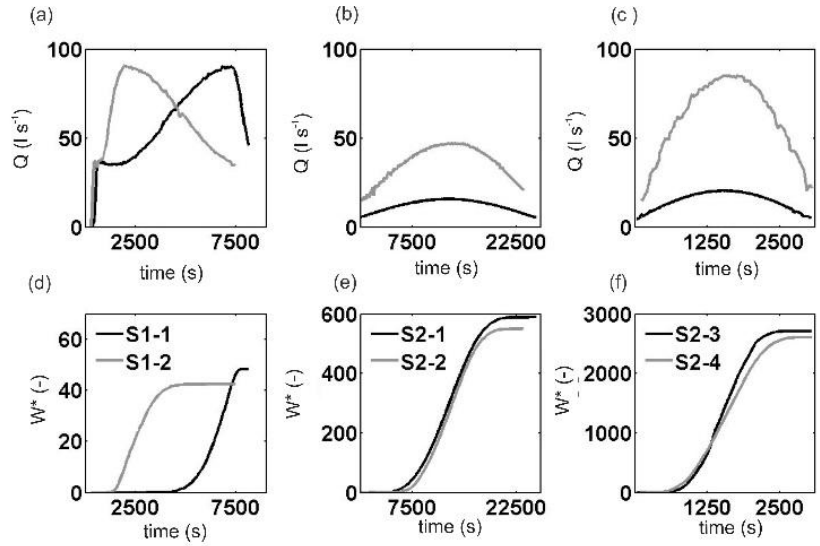

Fig. 1. Hydrographs (a), (b), and (c), and corresponding dimensionless, effective flow work on time for experiments of series S1 (d) and S2 with clear-water (e), and live-bed conditions (f)

3. Results

According to equation (5) the flow is represented by the dimensionless flow work, W*. To test such parameter for scaling scour, we compare the scour depth in Flume 1 with Sand 1 produced by two different hydrographs with the same W*. Figure 2 shows the dimensionless scour depth Z* over the dimensionless effective flow work W* for experiments of series S1.

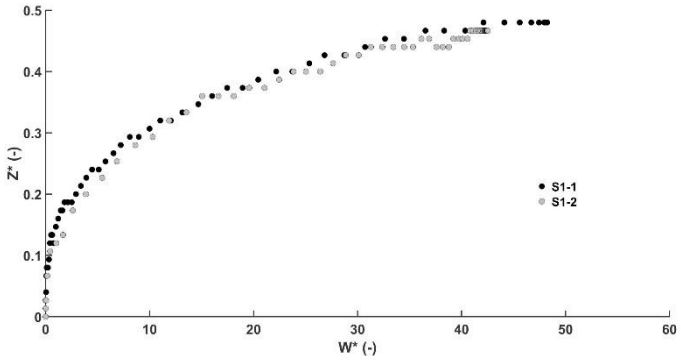

Fig. 2. Dimensionless scour depth over dimensionless effective flow work for experiments of series S1

The two hydrographs in experiments S1-1 and S1-2 produced the same relative scour depth for given values of W*, showing the uniqueness of the relation between both variables, and showing that W* is an appropriate parameter for representing the flow in scour phenomena.

The parameter representing the sediment bed in scour problems, D* was tested through experiments of series S2 under the clear-water (experiments S2-1 and S2-2) and the live-bed condition (experiments S2-3 and S2-4). Perfect similitude was achieved between systems in experiments S2-1 and S2-3 (Flume 1 and Sand 1) and S2-2 and S2-4 (Flume 2 and Polystyrene), i.e. $\lambda_{Z*} \cong \lambda_{W*} \cong \lambda_{D*} \cong \lambda_{D/d_s} \cong 1$, while the geometric scale was 1:3. Both sediments, Sand 1 and Polystyrene have a very similar dimensionless grain diameter of 18 and 20, respectively, and hydrographs in series 2 were designed in order to produce the same work in time. Figure 3 shows the relative scour depth over time, as well as Z* over W* for pairs of experiments with clear-water and live-bed conditions.

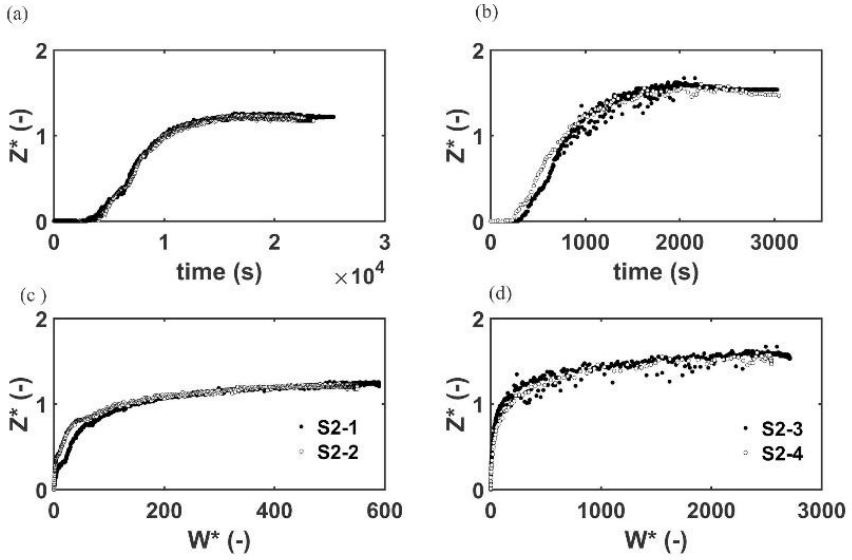

Fig. 3. Relative scour depth over time (a) and (b), and over W* for experiments S2-1 and S2-2 with clear-water condition (c) and for experiments S2-3 and S2-4 with live-bed conditions (d)

In experiments with live-bed conditions flow intensity achieved a peak value of 1.3, and thus sediment transport with bed-forms took place. From Fig. 4 it is evident that similitude of the scour process is obtained when controlling parameters in equation (5) are similar in model and prototype. Figure 4 shows the relative scour depth over the dimensionless, effective flow work for experiments of series S3. These experiments were conducted with constant discharge until advanced stages of scour. Experiments S3-1 and S3-2 were conducted with Sand 3 (D* =21) and Polystyrene (D*=20), respectively, while experiments S3-3 and S3-4 were conducted with Sand 4 and Acetal, both having identic D* = 40.

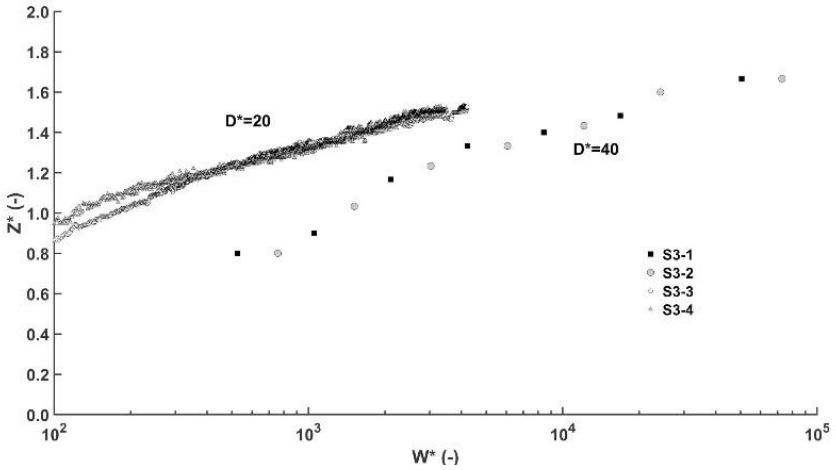

Fig. 4. Relative scour depth over dimensionless, effective flow work in series S3

Remarkably, similitude of the relative scour depth Z* was obtained in all experiments of series S3, with different hydrographs, piers and sediments, providing that $\lambda_{W*} \cong \lambda_{D*} \cong \lambda_{D/d_s} \cong 1$, confirming the reliability of the dimensionless grain diameter D* as an appropriate parameter representing the sediment bed in scaled bridge scour problems.

In the previous analyses perfect similitude of the controlling scales in the compared scour experiments was achieved according to equation (5), i.e. $\lambda_{Z*} \cong \lambda_{W*} \cong \lambda_{D*} \cong \lambda_{D/d_s} \cong 1$. This condition is rare, because to avoid contraction effects on pier scour, the flume width to pier size ratio is restricted to B / D > 8, consequently the typical flume width limits the diameter of the model pier leading to smaller values of D/d_s in the model than in the prototype. The effects of D/d_s on the scour depth have been extensively studied by [10, 15, 16]. Figure 5 show the relative scour depth Z* on the pier to sediment size ratio, D/d_s for three groups of sediments with similar W* and D*.

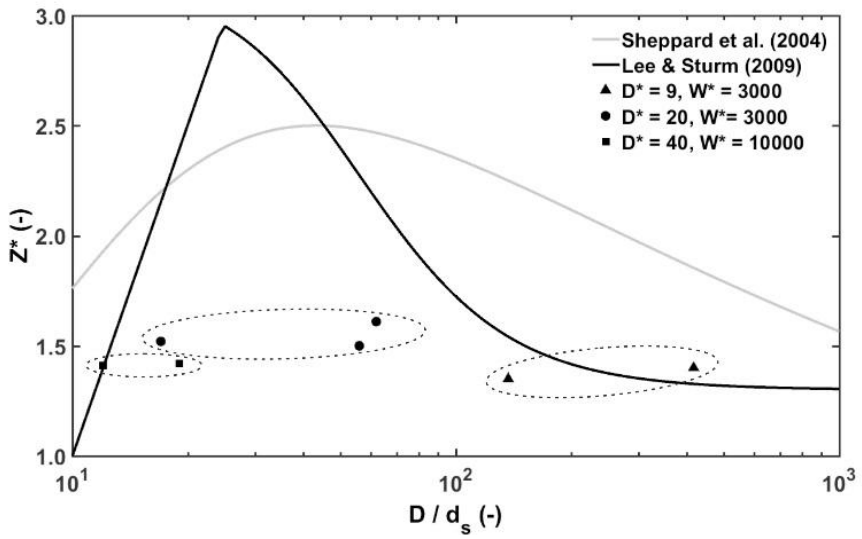

Fig. 5. Relative scour depth on the pier to sediment size ratio for experiments S5-1 and S5-2 ; S4-1, S4-3, and S5-3 ; and S3-1, and S3-3. The continuous lines correspond to the curves proposed by [15] and [10]

Remarkably, the scale effect in D/d_s -distorted models becomes of minor importance if D* and W* are similar in model and prototype.

4. Conclusion

The feasibility of physical modelling techniques for reliable quantification of prototype bridge pier scour in scale models was investigated through 17 ad-hoc designed laboratory experiments conducted in experimental installations having different flume, pier and sediment properties. Scour under clear-water and live-bed conditions caused by steady and unsteady discharges was analyzed.

The scales controlling scour similitude were the dimensionless effective flow work W*, and the dimensionless grain diameter D*.

Scale effects in D/d_s-distorted models are negligible, being the scour depth at the scale model a better estimator of prototype scour than scour depth computed by existent scour formulas.

Presented results show that the physical scale modelling of bridge pier scour is a suitable tool for scour estimations.

Acknowledgements

The presented results are part of the project Nr. 1150997: Bridge Pier Scour caused by Flood Waves, funded by the Chilean Research Council, CONICYT.

References

1. R. Bettess, Springer, Netherlands. (1990)
2. N. Cheng, Y.-M. Chiew, X. Chen, Journal of Engineering Mechanics, **142** (2016)
3. R. Ettema, G. Kirkil, M. Muste, Journal of Hydraulic Engineering, **132** (2006)
4. R. Ettema, B. Melville, B. Barkdoll, Journal of Hydraulic Engineering, **124** (1998)
5. B. Ettmer, F. Orth, O. Link, Journal of Hydraulic Engineering, **141** (2015)
6. S. Gorrick, J. Rodríguez, Journal of Hydro-Environment Research, **8** (2014)
7. J. Guo, Journal of Hydraulic Research **52** (2014)
8. V. Heller, Journal of Hydraulic Research, **49** (2011)
9. V. Heller, Journal of Hydraulic Research, **55** (2017)
10. S. Lee, T. Sturm, Journal of Hydraulic Engineering, **135** (2009)
11. O. Link, C. Castillo, A. Pizarro, A. Rojas, B. Ettmer, C. Escauriaza, S. Manfreda, Journal of Hydraulic Research, **55** (2017)
12. B. Melville, Journal of Hydraulic Engineering, **123** (1997)
13. A. Pizarro, B. Ettmer, S. Manfreda, A. Rojas, O. Link, Journal of Hydraulic Engineering, **143** (2017)
14. A. Raudkivi, Journal of Hydraulic Engineering, **112**, (1986)
15. D. Sheppard, M. Odeh, T. Glasser, Journal of Hydraulic Engineering, **130**, (2004)
16. M. Sheppard, B. Melville, H. Demir, Journal of Hydraulic Engineering, **140** (2014)
17. J. Thélusmond, L. Chevalier, B. DeVantier, International Journal of Hydrology Science and Technology, **3** (2013)
18. M. Yalin, J. Kamphuis, Journal of Hydraulic Research, **9** (1971)